

# Effect of Working Pressure on the Structural and Thermoelectric Properties of Bismuth Telluride Thin Films Deposited by Magnetron Sputtering



Zhiwei Zhang, Yuan Deng, Yao Wang, Daming Zhu, Wenhui Yan, Zhigang Jia and Fen Wang

**Abstract** Highly (001)-oriented bismuth telluride polycrystalline thin films were prepared on quartz glass by magnetron co-sputtering at appropriate working pressure. The effect of working pressure on the growth behavior, microstructure and electrical transport properties of  $\text{Bi}_2\text{Te}_3$  thin films were studied. The results showed that increasing working pressure brought more particle scattering and also decreased the velocity of the sputtered particles. As a result, the nucleation rate of the crystal grains decreased and more sufficient growth along the in-plane direction was induced. When the working pressure was 2.0 Pa, the balance between nucleation rate and growth rate of the crystal grains reached, which brings highly (001) crystal plane orientation in  $\text{Bi}_2\text{Te}_3$  polycrystalline thin film. Compared with the  $\text{Bi}_2\text{Te}_3$  thin film with certain (015) orientation deposited at 0.5 Pa, the

---

Z. Zhang (✉) · D. Zhu · W. Yan · Z. Jia · F. Wang  
AECC Aero Engine Academy of China, Beijing 101304, China  
e-mail: zzw704@163.com

D. Zhu  
e-mail: damingzhu@126.com

W. Yan  
e-mail: abuaa@163.com

Z. Jia  
e-mail: jia2001720@126.com

F. Wang  
e-mail: wafenn@163.com

Y. Deng · Y. Wang  
Beijing Key Laboratory for Advanced Functional Materials and Thin Film Technology,  
School of Materials Science and Engineering, Beihang University,  
Beijing 100191, China  
e-mail: dengyuan@buaa.edu.cn

Y. Wang  
e-mail: wang-yao@buaa.edu.cn

(001)-oriented  $\text{Bi}_2\text{Te}_3$  thin film had the double Seebeck coefficient, which was above  $-200 \mu\text{V K}^{-1}$  between 300 and 400 K and reached to the maximum value  $-225 \mu\text{V K}^{-1}$  at 360 K. Therefore the power factor of the thin film is greatly enhanced and reaches to above  $38 \times 10^{-4} \text{ W m}^{-1} \text{ K}^{-2}$  at 360 K, which is comparable to the value of the optimal  $\text{Bi}_2\text{Te}_{2.7}\text{Se}_{0.3}$  bulk alloys.

**Keywords** Bismuth telluride · Thin film · Magnetron sputtering  
Thermoelectric property

## Introduction

Thermoelectric (TE) materials can achieve the direct conversion between heat and electricity and have been heavily investigated over the past few decades for solid state cooling and power generation [1–3]. Energy conversion efficiency of a TE material can be evaluated by the dimensionless figure of merit  $ZT = S^2\sigma T/\kappa$ , where  $S$ ,  $\sigma$ ,  $T$  and  $\kappa$  are the Seebeck coefficient, electrical conductivity, absolute temperature and thermal conductivity, respectively [4, 5]. Therefore, a good TE material should possess high electrical conductivity, high Seebeck coefficient and low thermal conductivity. However, because these parameters are coupled via band structures and scattering mechanisms, it is difficult to control them independently and the optimization of thermoelectric property is limited in bulk materials [6]. Recently, low dimensionality has been proved to be an effective way to improve  $ZT$  by increasing the Seebeck coefficient due to quantum confinement effect and simultaneously decreasing thermal conductivity owing to the enhanced phonon scattering at boundaries and interfaces [7–10].

Bismuth telluride based thermoelectric materials are still the best TE materials near room temperature, which is very suitable for cooling and refrigeration. Based on the rapid development of micro-cooling devices integrated with microelectromechanical systems (MEMS), the deposition of high performance  $\text{Bi}_2\text{Te}_3$  based thin films is of great interest. Two dimensional thin films are also convenient for adjusting and optimizing the microstructure of TE materials [11]. Many techniques have been reported to prepare  $\text{Bi}_2\text{Te}_3$  based thin films, such as physical evaporation, molecular beam epitaxy (MBE), pulsed laser deposition (PLD), and metal organic chemical vapor deposition (MOCVD) [12–15]. Compared with these methods, magnetron sputtering is more beneficial to deposit thin films with high density and large-scale fabrication. During deposition, working pressure is a very important parameter, which can affect the deposition rate, quality and microstructure of thin film. Therefore, it is necessary to study the effect of working pressure on the microstructure and thermoelectric properties of  $\text{Bi}_2\text{Te}_3$  thin films particularly.

In this study,  $\text{Bi}_2\text{Te}_3$  thin films were deposited by co-sputtering in order to control the composition of the films. The effects of working pressure on the microstructure and thermoelectric properties of  $\text{Bi}_2\text{Te}_3$  thin films were investigated.

## Experimental

Bismuth telluride thin films were deposited on polished quartz glass substrate by co-sputtering method, described in our previous work [16]. Hot-pressed  $\text{Bi}_2\text{Te}_3$  target (99.99%) and Te target (99.99%) with 60 mm diameter were used and the distance between targets and substrates maintained at 90 mm.  $\text{Bi}_2\text{Te}_3$  target was connected to a direct current power supplier with 20 W and Te target was connected to a radio frequency power supplier with 45 W. The deposition temperature and duration were fixed at 350 °C and 1 h, while the working pressure varied from 0.5 to 2.2 Pa.

X-ray diffraction (XRD) patterns of the products were taken on a Rigaku D/MAX 2200 PC automatic X-ray diffractometer. Morphologies and composition of the thin films were analyzed by field emission scanning electron microscopy (FE-SEM) (FEI Sirion 200) and energy dispersive X-ray spectroscopy (EDS). Carrier concentration and mobility were measured on a Hall effect measurement system (ECOPIA HMS-3000). In-plane electrical conductivity and Seebeck coefficient were simultaneously measured by ZEM-3 (Ulvac Riko, Inc.).

## Results and Discussion

Figure 1 shows the XRD patterns of the  $\text{Bi}_2\text{Te}_3$  thin films deposited at different working pressure. It can be found that the diffraction peaks of the samples are well assigned to the standard pattern of  $\text{Bi}_2\text{Te}_3$  with rhombohedral structure (JCPDS 15-0863). For the  $\text{Bi}_2\text{Te}_3$  thin film deposited at 0.5 Pa, certain (015) orientation is achieved. Along with the increase of working pressure, the film gradually converts to be highly (001) oriented at 2.0 Pa, indicating the vital effect of working pressure on the microstructure of  $\text{Bi}_2\text{Te}_3$  thin film.

The surface view and cross-sectional view of the  $\text{Bi}_2\text{Te}_3$  thin films are shown in Fig. 2. From the surface view (Fig. 2a), it can be seen that the film deposited at 0.5 Pa consists of nanoscale grains with average size of about 600 nm. These grains are well crystallized, but not parallel to the substrate. From the cross-sectional view, it can be seen that the thin film has island growth mode with column structure, which are orderly stacked by nanoplates, as shown in Fig. 2b. This orientation is consistent with the result of XRD. As the working pressure increases, the films become more dense and flat composing of hexagonal crystals. As shown in Fig. 2g, h, the film deposited at 2.0 Pa is composed of 300 nm hexagonal crystals stacked orderly with the ab plane preferentially oriented to form columns normal to the substrate, which confirms the greatly enhanced intensity of (001) peaks as shown in XRD. For magnetron sputtering, increasing working pressure would bring more particle scattering and also decrease the velocity of the sputtered particles. As a result, the nucleation rate of crystal grains is decreased and more sufficient growth along the in-plane direction is induced. When the working pressure is 2.0 Pa, the

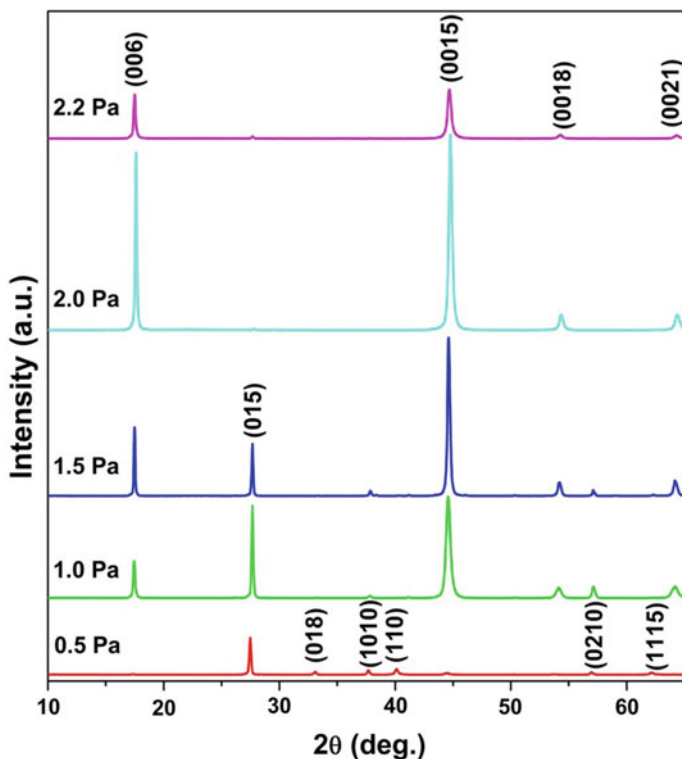


**Fig. 1** XRD patterns of the  $\text{Bi}_2\text{Te}_3$  thin films deposited at different working pressure

balance between nucleation rate and growth rate of crystal grains is reached, which brings highly (00 l) crystal plane orientation. All the films are stoichiometric with atomic ratio of  $\sim 2:3$ , as confirmed by EDS analysis (see Table 1 and the inset in Fig. 2).

Along with the structural characteristics, electrical transport properties of the  $\text{Bi}_2\text{Te}_3$  thin films were also strongly affected by the working pressure, as shown in Fig. 3. Figure 3a shows the change of room temperature carrier concentration and mobility with working pressure. Along with the increase of working pressure, carrier concentration of the films decreases gradually, which is about  $-2.9 \times 10^{20} \text{ cm}^{-3}$  at 0.5 Pa and decreases to  $-1.0 \times 10^{20} \text{ cm}^{-3}$  at 2.0 Pa. As evidenced by the SEM results, the lower nucleation rate and ampler growth of the crystal grains along the in-plane direction at higher working pressure would bring lower defects in the film and thus decrease the carrier concentration. On the contrary, carrier mobility of the films increases with working pressure, which achieves  $52 \text{ cm}^2 \text{ V}^{-1} \text{ s}^{-1}$  at 2.0 Pa. The gradually formed layered nanostructure and enhanced (001) plane orientation should constitute the transport passage for electrons. For the thin film deposited at 2.2 Pa, the weakened layered nanostructure and (001) plane orientation cause the decrease of carrier mobility.

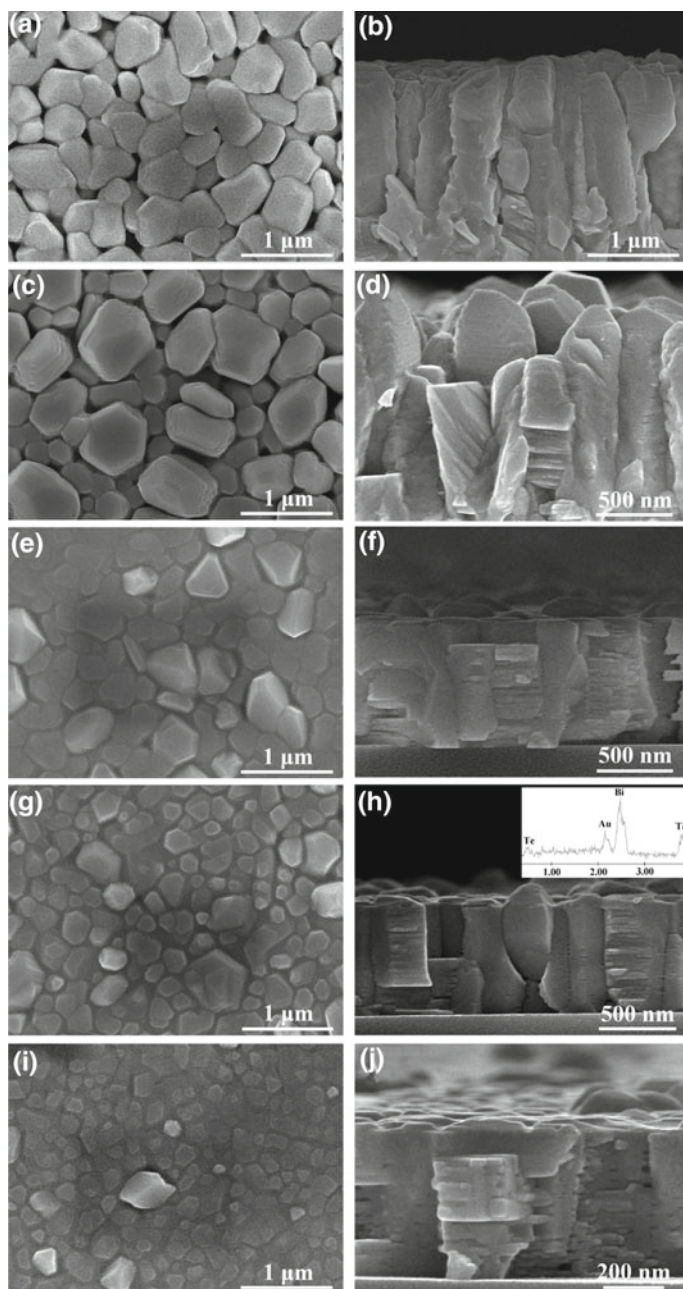


**Fig. 2** Surface view and cross-sectional view of the Bi<sub>2</sub>Te<sub>3</sub> thin films deposited at different working pressure: **a, b** 0.5 Pa; **c, d** 1.0 Pa; **e, f** 1.5 Pa; **g, h** 2.0 Pa; **i, j** 2.2 Pa

**Table 1** Chemical composition of the thin films analyzed by EDS

Working pressure (Pa)	Bi content (at.%)	Te content (at.%)
0.5	39.9	60.1
1.0	40.1	59.9
1.5	40.1	59.9
2.0	39.9	60.1
2.2	39.8	60.2

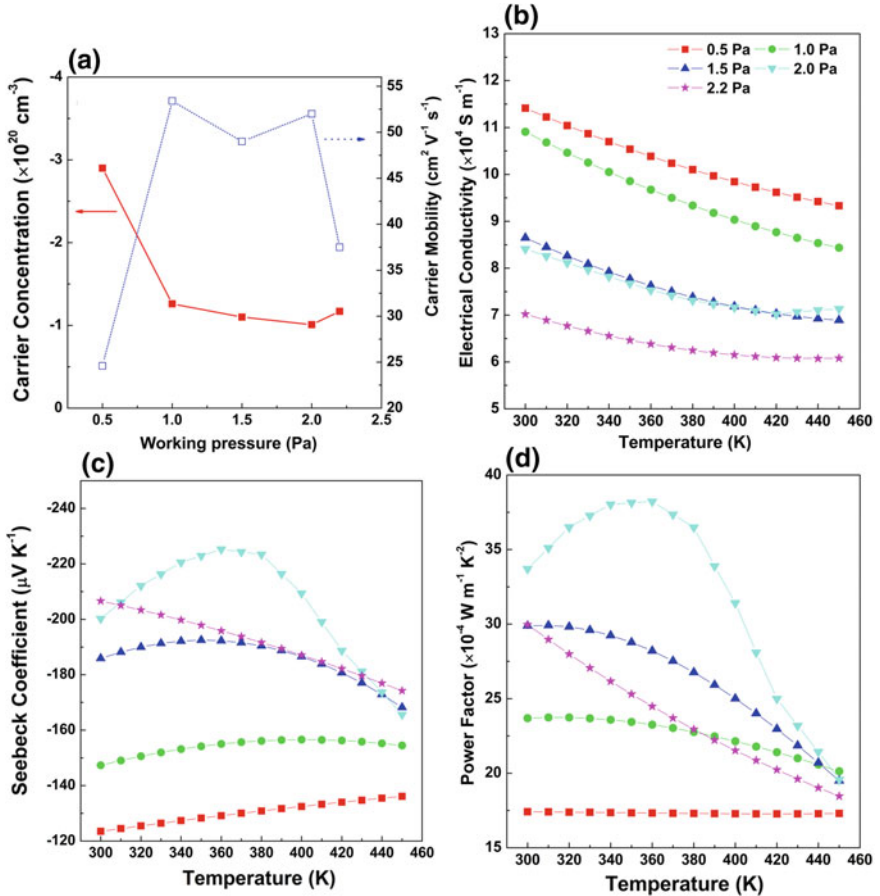


**Fig. 3** Room temperature carrier concentration, carrier mobility (a) and the temperature dependence of electrical conductivities (b), seebeck coefficients (c) and power factors (d) of the Bi<sub>2</sub>Te<sub>3</sub> thin films deposited at different working pressure with distinct microstructures

As shown in Fig. 3b, electrical conductivity decreases with the increase of working pressure. Electrical conductivity can be expressed with carrier concentration and mobility as  $\sigma = ne\mu$ , where  $n$ ,  $\mu$ , and  $e$  represent carrier concentration, carrier mobility, and the electronic charge, respectively. Therefore, the main reason is the decreased carrier concentration at higher working pressure. However, the electrical conductivity of the film deposited at 2.0 Pa is still comparable with the values of hot-pressed or SPS sintered  $\text{Bi}_2\text{Te}_3$  based bulk materials, which is about  $8.4 \times 10^4 \text{ S m}^{-1}$  at room temperature [17, 18].

Figure 3c shows the influence of working pressure on Seebeck coefficients of the thin films. All films have negative values of Seebeck coefficient, indicating the n-type transport behavior. With the rising working pressure, the absolute value of Seebeck coefficient increases and achieves the maximum value for the film deposited at 2.0 Pa, which is  $200 \mu\text{V K}^{-1}$  at room temperature and  $225 \mu\text{V K}^{-1}$  at 360 K. Because the carrier concentration and mobility of the films deposited between 1.0 and 2.0 Pa are nearly the same, the main reason should be the enhanced (001) plane orientation and more obvious layered nanostructure. Based on Boltzmann distribution for the electrons, the Seebeck coefficient can be expressed as  $S = k_B(s - \ln n)/e + C_1$ , where  $k_B$  is the Boltzmann constant,  $s$  is the scattering parameter and  $C_1$  is the proper constant [19]. As an approximation, the relaxation time can be expressed as  $\tau = \tau_0 E^s$ , where  $\tau_0$  is a constant and  $E$  stands for the energy of carriers. The preferential orientation of (001) plane and layered nanostructure parallel to the substrate would prolong relaxation time and enlarges scattering parameter. Therefore, the film deposited at 2.0 Pa with complete (001) plane orientation and obvious layered nanostructure has the maximum Seebeck coefficient.

The relationship between temperature and power factor for the films deposited at different working pressure is shown in Fig. 3d. For the film deposited at 2.0 Pa, the power factor is near  $34 \times 10^{-4} \text{ W m}^{-1} \text{ K}^{-2}$  and exceeds  $38 \times 10^{-4} \text{ W m}^{-1} \text{ K}^{-2}$ , which is even comparable with the reported maximum power factor of the n-type  $\text{Bi}_2\text{Te}_{2.7}\text{Se}_{0.3}$  bulk material ( $35 \times 10^{-4} \text{ W m}^{-1} \text{ K}^{-2}$ ), indicating the superiority of magnetron sputtering for depositing (001)-oriented  $\text{Bi}_2\text{Te}_3$  based TE material [20].

## Conclusion

In summary, highly (001) plane orientation in  $\text{Bi}_2\text{Te}_3$  thin film has been achieved by optimizing working pressure using a simple magnetron co-sputtering method. Higher working pressure brings more particle scattering and also decreases the velocity of the sputtered particles. As a result, the nucleation rate of the crystal grains is decreased and more sufficient growth along the in-plane direction is induced. When the balance between nucleation rate and growth rate of the crystal grains is reached, highly (001) crystal plane orientation in  $\text{Bi}_2\text{Te}_3$  polycrystalline

thin film is achieved. Due to this special nanostructure, the Seebeck coefficient and power factor of  $\text{Bi}_2\text{Te}_3$  thin film can be greatly promoted. Preferential orientation of the optimum crystal plane is also applicable to other TE materials with anisotropy for enhancing thermoelectric property.

**Acknowledgements** This work was supported by the State Key Program of National Natural Science Foundation of China (Grant No. 61534001) and National Natural Science Foundation of China (Grant No. 51601005)

## References

1. I. Chowdhury, R. Prasher, K. Lofgreen, G. Chrysler, S. Narasimhan, R. Mahajan, D. Koester, R. Alley, R. Venkatasubramanian, On-chip cooling by superlattice-based thin-film thermoelectrics. *Nat. Nanotechnol.* **4**, 235–238 (2009)
2. Q. Zhang, X. Huang, S. Bai, X. Shi, C. Uher, L. Chen, *Adv. Eng. Mater.* **18**, 194–213 (2016)
3. X. Hu, P. Jood, M. Ohta, M. Kunii, K. Nagase, H. Nishiate, M.G. Kanatzidis, A. Yamamoto, Power generation from nanostructured PbTe-based thermoelectrics: comprehensive development from materials to modules. *Energy Environ. Sci.* **9**, 517–529 (2016)
4. D.M. Rowe, *Thermoelectrics Handbook: Macro to Nano* (CRC Press, Boca Raton, 2005)
5. Y. Chen, M. He, B. Liu, G.C. Bazan, J. Zhou, Z. Liang, Bendable n-type metallic nanocomposites with large thermoelectric power factor. *Adv. Mater.* **29**, 1604752 (2017)
6. L.D. Zhao, V.P. Dravid, M.G. Kanatzidis, The panoscopic approach to high performance thermoelectrics. *Energy Environ. Sci.* **7**, 251–268 (2014)
7. Y. Pei, H. Wang, G.J. Snyder, Band engineering of thermoelectric materials. *Adv. Mater.* **24**, 6125–6135 (2012)
8. J.J. Urban, Prospects for thermoelectricity in quantum dot hybrid arrays. *Nat. Nanotechnol.* **10**, 997–1001 (2015)
9. Y. Liu, P. Sahoo, J.P.A. Makongo, X. Zhou, S.J. Kim, H. Chi, C. Uher, X. Pan, P.F. P. Poudeu, Large enhancements of thermopower and carrier mobility in quantum dot engineered bulk semiconductors. *J. Am. Chem. Soc.* **135**, 7486–7495 (2013)
10. D. Wu, L.D. Zhao, F. Zheng, L. Jin, M.G. Kanatzidis, J. He, Understanding nanostructuring processes in thermoelectrics and their effects on lattice thermal conductivity. *Adv. Mater.* **28**, 2737–2743 (2016)
11. M. Tan, Y. Deng, Y. Wang, Ordered structure and high thermoelectric properties of  $\text{Bi}_2(\text{Te}, \text{Se})_3$  nanowire array. *Nano Energy* **3**, 144–151 (2014)
12. M. Kashiwagi, S. Hirata, K. Harada, Y. Zheng, K. Miyazaki, M. Yahiro, C. Adachi, Enhanced figure of merit of a porous thin film of bismuth antimony telluride. *Appl. Phys. Lett.* **98**, 023114 (2011)
13. N. Peranio, M. Winkler, M. Dürschnabel, J. König, O. Eibl, Assessing antisite defect and impurity concentrations in  $\text{Bi}_2\text{Te}_3$  based thin films by high-accuracy chemical analysis. *Adv. Funct. Mater.* **23**, 4969–4976 (2013)
14. A. Li Bassi, A. Bailini, C.S. Casari, F. Donati, A. Mantegazza, M. Passoni, V. Russo, C.E. Bottani, Thermoelectric properties of Bi–Te films with controlled structure and morphology. *J. Appl. Phys.* **105**, 124307 (2009)
15. Z. Sun, S. Liufu, X. Chen, L. Chen, Enhanced thermoelectric properties of  $\text{Bi}_{0.5}\text{Sb}_{1.5}\text{Te}_3$  films by chemical vapor transport process. *ACS Appl. Mater. Interfaces* **3**, 1390–1393 (2011)
16. Z. Zhang, Y. Wang, Y. Deng, Y. Xu, The effect of (001) crystal plane orientation on the thermoelectric properties of  $\text{Bi}_2\text{Te}_3$  thin film. *Solid State Commun.* **151**, 1520–1523 (2011)



17. L.P. Hu, X.H. Liu, H.H. Xie, J.J. Shen, T.J. Zhu, X.B. Zhao, Improving thermoelectric properties of n-type bismuth–telluride-based alloys by deformation-induced lattice defects and texture enhancement. *Acta Mater.* **60**, 4431–4437 (2012)
18. J.S. Son, M.K. Choi, M.K. Han, K. Park, J.Y. Kim, S.J. Lim, M. Oh, Y. Kuk, C. Park, S. J. Kim, T. Hyeon, *Nano Lett.* **12**, 640–647 (2012)
19. D.B. Hyun, J.S. Hwang, J.D. Shim, Thermoelectric properties of  $(\text{Bi}_{0.25}\text{Sb}_{0.75})_2\text{Te}_3$  alloys fabricated by hot-pressing method. *J. Mater. Sci.* **36**, 1285–1291 (2001)
20. X. Yan, B. Poudel, Y. Ma, W.S. Liu, G. Joshi, H. Wang, Y.C. Lan, D.Z. Wang, G. Chen, Z.F. Ren, Experimental studies on anisotropic thermoelectric properties and structures of n-type  $\text{Bi}_2\text{Te}_{2.7}\text{Se}_{0.3}$ . *Nano Lett.* **10**, 3373–3378 (2010)